Vol 18 No 4, April 2009
1674-1056/2009/18(04)/1443-08
Chinese Physics B
© 2009 Chin. Phys. Soc.
and IOP Publishing Ltd

Studies of K-shell x-ray energy shifts induced by MeV/u heavy ions*

Song Zhang-Yong(宋张勇)[a)†], Yang Zhi-Hu(杨治虎)[a)], Shao Jian-Xiong(邵剑雄)[b)], Cui Ying(崔 莹)[b)], Zhang Hong-Qiang(张红强)[b)], Ruan Fang-Fang(阮芳芳)[a)], Du Juan(杜 鹃)[b)], Gao Zhi-Min(高志民)[b)], Yu De-Yang(于得洋)[a)], Chen Xi-Meng(陈熙萌)[b)], and Cai Xiao-Hong(蔡晓红)[a)]

[a)] *Institute of Modern Physics, the Chinese Academy of Sciences, Lanzhou* 730000, *China*

[b)] *School of Nuclear Science and Technology, Lanzhou University, Lanzhou* 730000, *China*

(Received 14 July 2008; revised manuscript received 21 August 2008)

This paper reports that the K x-ray spectra of the thin target $_{47}$Ag, $_{48}$Cd, $_{49}$In and $_{50}$Sn were measured by an HPGe semi-conductor detector in collisions with 84.5 MeV $_6C^{4+}$ ions. Our experiment revealed the $K\alpha$ x-ray energy shifts were not obvious and the $K\beta_1$ x-ray energy shifts were about 90∼110 eV. The simple model of Burch *et al* has been previously used to calculate the K x-ray energy shifts due to an additional vacancy in $2p$ orbit. The present work extends the model of Burch to calculate the x-ray energy shifts of multiple ionized atoms induced by heavy ions with kinetic energy of MeV/u. In addition to our experimental results, many other experimental results are compared with the calculated values by using the model.

Keywords: K-shell x-ray energy shifts, heavy ion collisions, multiple ionization
PACC: 3120B, 3220R, 3450H

1. Introduction

Atomic inner-shell ionization studies have progressed over the last four decades in collisions of MeV/u heavy ions with atoms. The experimental method is mostly to measure the x-ray spectra induced in collisions. A common feature of these measurements is that the x-ray spectra shift to higher energies with respect to corresponding x-ray energies for singly ionized atoms. For instance, Patrick Richard *et al* reported the characteristic $K\beta$ x-ray energy shifts of $_{28}$Ni and $_{29}$Cu as produced by 15 MeV $_8O^{4+}$ ion bombardments for the first time in 1969.[1] They found that the $K\beta$ x-ray spectra shifted by 112±15 and 97±15 eV respectively, are relative to energies produced by x-ray and proton excitation. Burch *et al* measured the K x-ray spectra of $_{20}$Ca and $_{23}$V as produced by 15 MeV $_8O^{4+}$ ion bombardments in 1970. Their experimental results revealed that the $K\alpha$ and $K\beta$ lines shifted approximately by 54 and 157 eV, are relative to the proton-induced spectra.[2] Li *et al* studied the $K\alpha$ and $K\beta$ x-ray energy shifts of $_{29}$Cu as induced by 75 MeV $_{28}Ni^{q+}$ ions, which were about 61 and 170 eV.[3] Several research groups have studied the x-ray energy shifts and multiple ionization effects on atomic parameters in heavy-ion collisions from 1970s to 1990s.[4]

From the above description, we can see that some of the literature observed simultaneously the $K\alpha$ and $K\beta$ x-ray energy shifts, but some observed only the $K\beta$ x-ray energy shifts. In heavy-ion collisions, the x-ray energy shifts are interpreted as the result of additional vacancies in outer shells, i.e. the multiple ionization of target atoms, which depend on the kinetic energy E_1 and the effective charge $Z_1^{\rm eff}$ of the incident ions. For example, in 1976, Wheeler *et al* [5] studied x-ray energy shifts of $_{20}$Ca, $_{21}$Sc, $_{22}$Ti, $_{23}$V, $_{26}$Fe, $_{28}$Ni, $_{29}$Cu, $_{30}$Zn, $_{32}$Ge, $_{37}$Rb, $_{38}$Sr, $_{39}$Y, $_{40}$Zr, and $_{46}$Pd induced by carbon ions in energy ranges of 8∼36 MeV. They expected the maximum x-ray energy shifts occurring at the point where the incident projectile velocity matched the average velocity of the L-shell electrons, however, the maximum energy shifts for $_{20}$Ca, $_{22}$Ti, $_{26}$Fe and $_{30}$Zn occurred approximately at $E_1/\lambda\overline{U}_L^{\rm eff}$=1.2, 1.1, 0.9, and 0.6, respectively. In 1996, Fazinić[6] studied the K-shell ionization of $_{23}$V, $_{24}$Cr, $_{25}$Mn, $_{26}$Fe, $_{27}$Co $_{28}$Ni, and $_{29}$Cu by 5–12 MeV carbon ions. They found the maximum K x-ray en-

*Project supported by the National Natural Science Foundation of China (Grant No 10774149).
†E-mail: songzhy@impcas.ac.cn

ergy shifts occurring at the maximum kinetic energy $E_1 = 12\,\mathrm{MeV}$, and the minimum energy shifts occurring at $E_1 = 5\,\mathrm{MeV}$. From their experimental results, it also can be seen that the $K\alpha$ and $K\beta$ x-ray energy shifts decreased monotonically as the Z_2 (target atomic number) increased. In approximate symmetric ion–atom collisions ($Z_2/Z_1 \approx 1$), Laubert *et al* measured the K-shell x-ray spectra in collisions of $_{13}$Al-$_{13}$Al and $_{28}$Ni-$_{28}$Ni systems in energy ranges from 500 keV to 40 MeV in 1975.[7] Their results indicated that the $K\alpha$ x-ray energy shifts became larger and larger as incident kinetic energy increased until the maximum incident energy of 40 MeV. In 2005, Ciortea *et al* [8] used heavy ions of $_{26}$Fe, $_{27}$Co, and $_{28}$Ni to interact with $_{21}$Sc and $_{29}$Cu target in energy ranges of 0.2∼1.75 MeV/u. Their experimental results indicated that both incident ions and targets' K x-ray energy shifts monotonically increased with the incident energies. They also found the similar results in non-symmetric heavy-ions collisions.[9]

In theory, Burch *et al* introduced a simple potential model approach for calculating K-shell x-ray energy shifts due to an additional vacancy in $2p$ shell in 1974.[10] This model had been extended to arbitrary defect configuration[11] and to relativistic energy level.[12] In collisions of heavy ions with atoms the strong Coulomb field of the projectile can cause simultaneous ejection of several electrons with relatively high probabilities, i.e. multiple ionization effects. As a result of the multiple ionization instead of a single-hole x-ray transition, named the diagram line, the x-rays are considerably shifted, with respect to corresponding x-ray energies for singly ionized atoms. In the past few years Banaś *et al* studied the multiple ionization effects by fitting the x-ray spectra measured by a semiconductor detector with their proposed model.[13]

In the present work, the model of Burch *et al* for calculating K x-ray energy shifts due to an additional vacancy in $2p$ shell was extended for calculating the x-ray energy shifts of multiply ionized atoms by MeV/u heavy ions. The model just considered the contribution of direct electron–electron Coulomb potential energy to the shifts of binding energy of $2p$ and $3p$ shells. The contribution of electron–nuclear potential energy due to a reduction of nuclear charge screening and the electron–electron exchange potential energies to the shifts of binding energy were neglected. The vacancy rearrangements during the time from collisions to x-ray emission were not included in the model. The present work measured the K-shell x-ray spectra of foil target $_{47}$Ag, $_{48}$Cd, $_{49}$In and $_{50}$Sn induced by 84.5 MeV carbon ions with an HPGe semiconductor detector. Our experimental results indicated that the $K\alpha$ x-ray energy shifts were not obvious, but the $K\beta_1$ x-ray energy shifts were about 90∼110 eV. In addition to our experimental results, lots of other experimental results in literatures were examined and compared with the theoretical values calculated by our model. The calculated results agreed well with the experimental results at larger ranges of Z_2/Z_1.

2. Theoretical model

The theoretical model used in this paper for calculating the K x-ray energy shifts of multiply ionized atoms is constructed based on the simple model of Burch *et al*.[10] The model of Burch was originally used to calculate the K x-ray energy shifts due to an additional $2p$ vacancy and was performed some extensions by Talukdar *et al* [11,12,14] Burch and Talukdar *et al* assumed that removal of a $2p$ electron increased the binding energy of each of the levels, such as $1s$, $2p$ and $3p$ orbits. The shifts of the binding energy were given by (they did not consider the spin-orbit coupling energy)

$$\begin{aligned}\delta E_{1s}^{\mathrm{dir}} &= \langle 1s \mid V_{2p}^{\mathrm{dir}} \mid 1s\rangle \\ &= \int_0^{+\infty}\int_0^{+\infty} \frac{1}{r_>} \mid P_{1s}(r_1)\mid^2 \mid P_{2p}(r_2)\mid^2 \mathrm{d}r_1\mathrm{d}r_2 \\ &= F^0(1s2p), \end{aligned} \tag{1}$$

$$\begin{aligned}\delta E_{2p}^{\mathrm{dir}} &= \langle 2p \mid V_{2p}^{\mathrm{dir}} \mid 2p\rangle \\ &= \int_0^{+\infty}\int_0^{+\infty} \frac{1}{r_>} \mid P_{2p}(r_1)\mid^2 \mid P_{2p}(r_2)\mid^2 \mathrm{d}r_1\mathrm{d}r_2 \\ &= F^0(2p2p), \end{aligned} \tag{2}$$

$$\begin{aligned}\delta E_{3p}^{\mathrm{dir}} &= \langle 3p \mid V_{2p}^{\mathrm{dir}} \mid 3p\rangle \\ &= \int_0^{+\infty}\int_0^{+\infty} \frac{1}{r_>} \mid P_{3p}(r_1)\mid^2 \mid P_{2p}(r_2)\mid^2 \mathrm{d}r_1\mathrm{d}r_2 \\ &= F^0(2p3p). \end{aligned} \tag{3}$$

where V_{2p}^{dir} is the direct electron–electron Coulomb potential energy produced by a $2p$ vacancy. Burch *et al* used the sudden approximation to define the transition energies as differences in binding energies. The x-ray transition energy shifts were given by

$$\delta K\alpha^{\mathrm{dir}}(2p) = \delta E_{1s}^{\mathrm{dir}} - \delta E_{2p}^{\mathrm{dir}}, \tag{4}$$

$$\delta K\beta^{\mathrm{dir}}(2p) = \delta E_{1s}^{\mathrm{dir}} - \delta E_{3p}^{\mathrm{dir}}. \tag{5}$$

Bhattacharya *et al* gave a clear picture of the error involved in the model of Burch *et al* by comparing

with the traditional theoretical approach (TTA),[14] and they found that the error can be neglected. In fact Burch *et al* just considered the direct Coulomb potential in their approach, but in TTA the direct and exchange Coulomb potential were both included.

Because the contribution of exchange potential is very small (about 3 eV), we will only consider the direct potential energy in the present work. As there is a $2p$ vacancy, not only the direct electron–electron Coulomb interaction could increase the binding energy of $2p$ and $3p$ shell, but also the electron–nuclear interaction could increase the binding energy due to a reduction of the nuclear charge screening. We applied the Hartree–Fock approximation method to calculate the electron–nuclear interactional contribution to the binding energy, and found that it was about 2 eV, so this contribution can be neglected too. Here we also use the sudden approximation to define the differences in binding energies as the x-ray transition energies. Only considering the direct contribution of electron–electron Coulomb potential energy, we find that the transition energy shifts for $K\alpha$ and $K\beta$ are slightly larger than the values of TTA and including electron–nuclear contribution.

In MeV/u heavy-ion collisions, the target atoms are always multiply ionized. According to the independent electron model of multiple ionization, the probability for producing n vacancies in $2l$ ($l = s$ or p) shell is $P_{2l}(n) = C_N^n p_{2l}^n (1 - p_{2l})^{N-n}$, where p_{2l} is the ionization probability per electron at the moment of collisions. One assumes a constant K x-ray energy shifts per an additional vacancy in $2l$ sub-shell and the contributions of vacancies in outer M, N, etc., shells are neglected. Thus the K x-ray energy shifts can be expressed as

$$\Delta K\alpha = n\delta K\alpha(2p) + m\delta K\alpha(2s), \quad (6)$$

$$\Delta K\beta = n\delta K\beta(2p) + m\delta K\beta(2s), \quad (7)$$

where $\delta K\alpha$ and $\delta K\beta$ are the x-ray energy shift per vacancy, n and m are the number of vacancy in $2p$ and $2s$ sub-shell respectively. In the heavy-ions collisions if the x-ray spectra were measured by a semi-conductor detector, the x-ray energy shifts would be the mean values of Eqs.(6) and (7):

$$\langle \Delta K\alpha \rangle = 6p_{2p}\delta K\alpha(2p) + 2p_{2s}\delta K\alpha(2s), \quad (8)$$

$$\langle \Delta K\beta \rangle = 6p_{2p}\delta K\beta(2p) + 2p_{2s}\delta K\beta(2s). \quad (9)$$

It can be seen from Eqs.(8) and (9) that the measured K x-ray energy shifts just depend on the ionization probabilities per electron p_{2l} and p_{2s}, which are related to the kinetic energy of projectile and the projectile–target combinations. Sulik *et al* [15] proposed a geometrical model (GM), which was constructed in the frame of binary encounter approximation (BEA) approach, for studying the multiple ionization in MeV/u heavy ions collisions. It is very well in describing the energetic heavy-ion collisions. Recently Lapicki[16] evaluated the GM model for studying multiple ionization in heavy-ions collisions. In the present work, the GM model was used to calculate the ionization probabilities per electron p_{2p} and p_{2s}. The x-ray energy shifts per vacancy $\delta K\alpha(2s)$, $\delta K\alpha(2p)$, $\delta K\beta(2s)$ and $\delta K\beta(2p)$ were calculated by using the model of Burch. Thus the K x-ray energy shifts $\langle \Delta K\alpha \rangle$ and $\langle \Delta K\beta \rangle$ were calculated according to Eqs.(8) and (9).

3. Experimental setup

The experiment was performed at the HIRFL in the National Laboratory in China. Ions of ${}_6C^{4+}$(84.5 MeV) were used for this measurement. The beam passed through an aperture of 2 mm in diameter and the beam spotted on the target, placed at 45° with respect to the beam, was about 3 mm. An HPGe detector having a resolution of 180 eV at 5.9 keV was located at 90° to the beam, and simultaneous measurement of the back scattered projectile was done with two Si surface barrier detectors kept at an angle 135° to the beam. During the measurements, periodic energy and FWHM calibration with radioactive sources (^{55}Fe and ^{241}Am) were done, and we estimated the absolute x-ray energy with the uncertainty of ±10 eV. The thickness of thin ${}_{47}$Ag, ${}_{48}$Cd, ${}_{49}$In, and ${}_{50}$Sn targets was about 180 ∼ 220 mg/cm^2. The target and particle detector were housed in a scattering chamber which was kept at a vacuum of 10^{-7} mb by a turbo molecular pump. A layer of Mylar was adhered inside the chamber in the interest of decreasing the background radiation. The HPGe detector was placed outside the scattering chamber which contained a 0.05 mm Beryllium window. The x-ray spectra and the backscattered projectiles were collected simultaneously on separate analogue-to-digital converters. The average beam current was about 0.5∼1 nA.

4. Results and discussion

The experimental K x-ray spectra are shown in Fig.1. They were analysed with a nonlinear fitting method by assuming a Gaussian line shape for the full energy x-ray peaks and a binomial background,

$$y = y_0 + A * \exp\left(-\frac{(x - x_c)^2}{2 * \omega^2} \right). \qquad (10)$$

Here, y_0 represents the binomial background, ω is the standard deviation of the peak (ω = FWHM/(2 $*$ $\sqrt{\ln 4}$)). We must say that the present work found the broadening of K x-ray spectral lines being not significant, so ω can be calculated approximately according to the energy and FWHM calibration results. Then there are only two free fitting parameters in our method of analysis of the low-resolution x-ray spectra, i.e. A and x_c. As shown in Fig.1, the fitting curves of $K\alpha$ x-ray lines of $_{47}$Ag, $_{48}$Cd, $_{49}$In, and $_{50}$Sn agreed with the experimental data very well, and the intensity ratio of $K\alpha_1$ to $K\alpha_2$ was about $2 \sim 3$ as shown

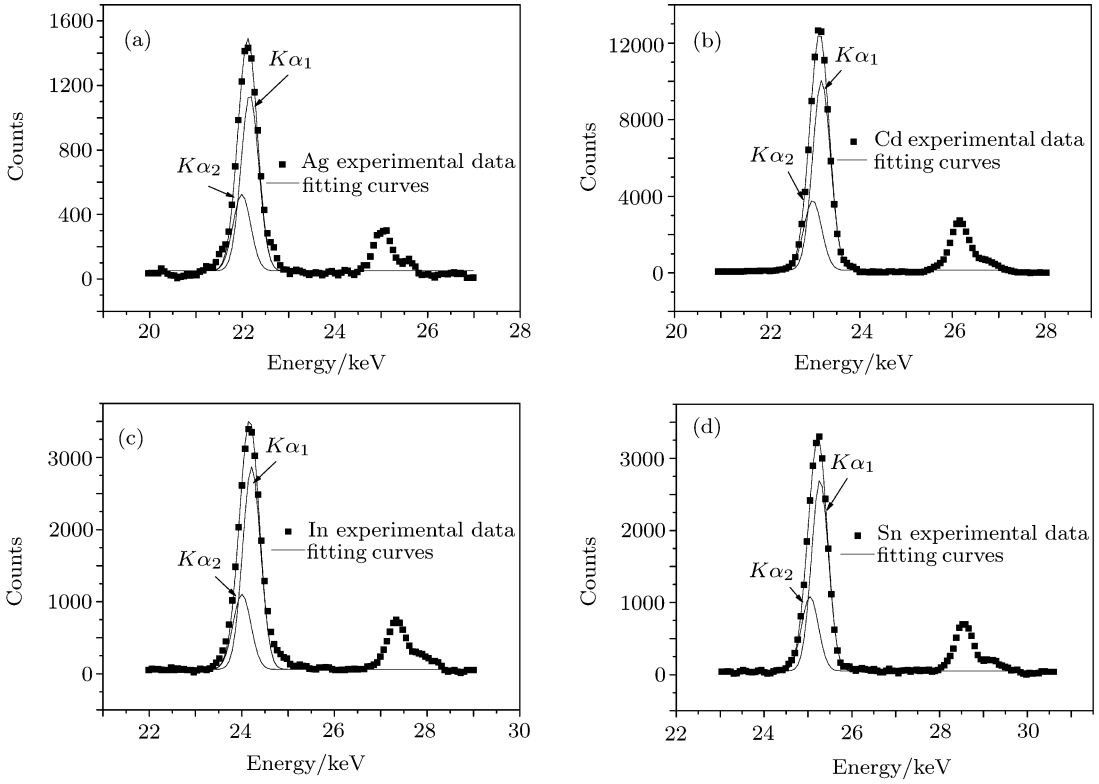


Fig.1. The experimental x-ray spectra of $_{47}$Ag, $_{48}$Cd, $_{49}$In, and $_{50}$Sn induced by 84.5 MeV carbon ions. It can be seen that the fitting curves agreed very well with the experimental data for $K\alpha$ x-ray.

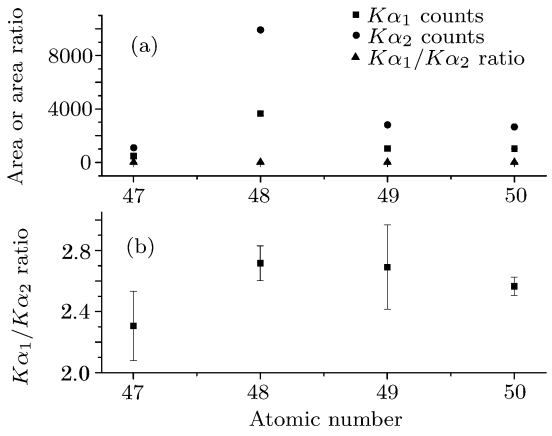


Fig.2. Intensities of $K\alpha_1$ and $K\alpha_2$ x-ray spectra. Figure 2(b) is magnified figure for the intensity ratio of $K\alpha_1$ and $K\alpha_2$.

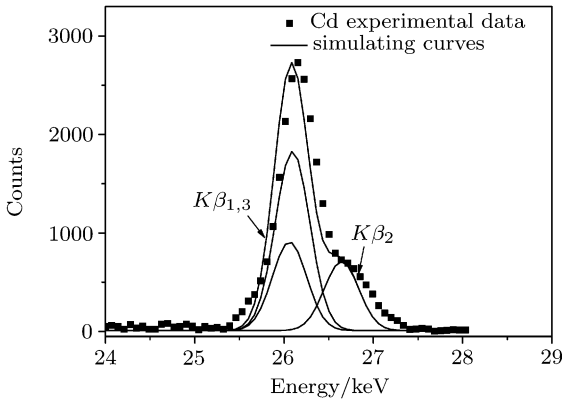


Fig.3. A typical $K\beta$ x-ray spectrum of $_{48}$Cd. It can be seen that the experimental spectrum shifts to higher energies relative to the simulating spectrum.

in Fig.2. Beyond all expectations, the fitting values of $K\alpha$ x-ray lines came near the diagram lines tabulated by Bearden,[17] but the $K\beta_1$ x-ray lines shifted to higher energies by about 90∼110 eV, relative to the diagram lines. Our experimental x-ray energy shifts, relative to the tabulated values in Ref.[17] were listed in Table 1. Figure 3 showed a simple simulating spectra of $K\beta$ x-ray of $_{48}$Cd, where x_c represent energies of diagram lines, for comparing with experimental spectra. The experimental results show that the shift of $K\alpha$ x-ray energy is not obvious whereas $K\beta$ x-ray energies significantly shift to higher energies are completely in accordance with the results of early literature.[1]

Table 1. The experimental x-ray energy shifts relative to the tabulated values[17] in our experiment, units in eV.

reaction	E_1/MeV	$\Delta E_{K\alpha}$	$\Delta E_{K\beta 1}$
$_6$C+$_{47}$Ag	84.5	–	112±7
$_6$C+$_{48}$Cd	84.5	–	94±5
$_6$C+$_{49}$In	84.5	–	96±4
$_6$C+$_{50}$Sn	84.5	–	94±3

In order to systematically study the relationship between x-ray energy shifts, kinetic energy of incident ions and projectile–target combination, our experimental results and lots of other experimental results in literatures were examined and compared with the theoretical values of our model.

For the purpose of calculating the K x-ray energy shifts for different projectile–target combinations according to Eq.(4) in heavy-ion collisions, firstly we estimated the values of x-ray energy shifts per vacancy, $\delta K\alpha$ and $\delta K\beta$, by using the RCN program written originally by Cowan.[18] This program is a self-consistent-field (SCF) iterative method and could be used to calculate the radial functions for each of any number of specified electron configurations, and any of radial Coulomb integrals could also be calculated, using the Hartree–Fock or any of several more approximate methods. The $F^0(1s2s)$, $F^0(2s2p)$, $F^0(2s3p)$ and $F^0(1s2p)$, $F^0(2p2p)$, $F^0(2p3p)$ for the $_{20}$Ca $(1s2s^2 \ldots 4s^2)$ ($\ldots$ refer to full shells), $_{23}$V $(1s2s^2 \ldots 3d^3 4s^2)$ *et al* were calculated for present problems. The calculated results of $\delta K\alpha$, $\delta K\beta$ and some other results were listed in Table 2. For $_{20}$Ca, $_{25}$Mn, $_{30}$Zn and $_{50}$Sn, our calculated values are slightly bigger than the results of Bhattacharya *et al*,[14] which is not beyond prospective as pointed out in Section 2.

Table 2. Calculated K x-ray energy shifts per $2l$ vacancy. It can be seen that for $_{47}$Ag, $_{48}$Cd, $_{49}$In, and $_{50}$Sn the values of $\delta K\beta$ is about three times of the $\delta K\alpha$, units in eV.

Target	$\delta K\alpha(2p)$	$\delta K\beta(2p)$	$\delta K\alpha(2s)$	$\delta K\beta(2s)$
$_{20}$Ca	30.47 or 28.04[12]	82.15	25.03	71.18
$_{22}$Ti	33.86	91.26	27.71	78.63
$_{23}$V	35.50	95.75	29.05	82.40
$_{24}$Cr	37.26	100.78	30.40	86.62
$_{25}$Mn	38.9 or 36.9[12]	105.0	31.77	90.03
$_{26}$Fe	40.53	109.48	33.14	93.87
$_{27}$Co	42.3	114.1	34.52	97.74
$_{28}$Ni	43.93	118.73	35.91	101.63
$_{29}$Cu	45.7	123.77	37.31	105.90
$_{30}$Zn	47.46or45.92[12]	128.11	38.72	109.47
$_{47}$Ag	77.52	200.20	64.59	171.58
$_{48}$Cd	79.29	204.55	66.26	175.50
$_{49}$In	81.20	209.04	67.95	179.46
$_{50}$Sn	82.96 or 80.32[12]	213.39	69.66	183.45

It can be seen from Table 2 that the $K\beta$ x-ray energy shifts per $2l$ vacancy of $_{47}$Ag, $_{48}$Cd, $_{49}$In and $_{50}$Sn are approximately three times of the $K\alpha$ x-ray energy shifts, which are about 65 eV for an additional $2s$ vacancy and 80 eV for a $2p$ vacancy, which is discrepant with our experimental results.

Secondly, the GM model[15] was used to estimate the ionization probability per electron p_{2l}. The GM model assumed the target electron to be ejected only if it was found inside a cylinder along the projectile trajectory within which the target electron acquired an amount of energy $E \geqslant I_{nl}$. According to the Binary-Encounter-Approximation (BEA), the value of the radius of the cylinder can be written as

$$b_0 = Z_1^{\text{eff}}/v_1 \times V[2G(V)/I_{nl}]^{1/2}. \tag{11}$$

where I_{nl} is the ionization energy of target electron, $V = v_1/v_2$ is the scaling velocity and $v_2 = [2I_{nl}]^{1/2}$ is velocity of target electron, $G(V)$ is the BEA scaling function, Z_1^{eff} is the effective charge of incident ions, which was determined based on the paper of Witikower *et al.*[19] It must be pointed out that the calculated x-ray energy shifts critically depend on the effective charge (or average equilibrium charge) of incidence through targets. The probability of ionization per electron was given by the GM model

$$p_{nl}(0, b_0) = \int_0^{+\infty} \mathrm{d}r r^2 R_{nl}^2 \beta(r, I_{nl}), \tag{12}$$

where R_{nl} is the radial part of the wavefunction and $\beta(r, I_{nl})$ is the relative surface of the spheres of radius r and it is related to the b_0.[15] For integrating Eq.(12), the hydrogenic functions were included in this paper.

At last the calculated ionization probability per electron and x-ray energy shifts based on the Eqs.(8) and (9) for all the projectile–target combinations were listed in Table 3, which included a lot of other experimental results and ours.

Table 3. The comparison of experimental data with the calculated values using the model, units in eV.

reaction	E_1/MeV	Z_2/Z_1	ΔE^{exp}		ΔE^{theo} (Gryzinski)			ΔE^{theo}(Gerjuoy *et al*)		
			$K\alpha$	$K\beta$	$K\alpha$	$K\beta$	p_L	$K\alpha$	$K\beta$	p_L
$_{28}$Ni+$_{29}$Cu	75	1.036	61[3]	170[3]	61.04	166.45	0.1722	88.69	241.63	0.2493
$_{26}$Fe+$_{29}$Cu	11.2	1.115	15[8]	110[8]	41.51	113.31	0.1177	58.18	158.63	0.1640
$_{26}$Fe+$_{29}$Cu	98	1.115	130[8]	420[8]	139.77	381.07	0.3942	150.93	411.66	0.4694
$_{8}$O+$_{20}$Ca	15	2.5	54±6[2]	158±6[2]	68.91	187.10	0.2906	92.46	251.14	0.3905
$_{8}$O+$_{23}$V	15	2.875	52±6[2]	156±6[2]	60.63	164.66	0.2197	87.22	236.83	0.3159
$_{6}$C+$_{20}$Ca	8	3.333	43[5]	110[5]	42.39	115.14	0.1790	60.15	163.29	0.2534
$_{6}$C+$_{20}$Ca	36	3.333	55[5]	160[5]	55.48	150.72	0.2344	63.35	172.11	0.2677
$_{8}$O+$_{28}$Ni	15	3.5	–	112±15[1]	47.05	128.11	0.1385	69.31	188.50	0.2030
$_{8}$O+$_{29}$Cu	15	3.625	–	97±15[1]	44.83	122.34	0.1270	66.13	180.28	0.1864
$_{6}$C+$_{22}$Ti	8	3.667	35[5]	110[5]	36.45	99.04	0.1391	52.36	142.10	0.1988
$_{6}$C+$_{22}$Ti	36	3.667	52[5]	158[5]	52.78	143.35	0.2011	66.73	181.15	0.2538
$_{6}$C+$_{23}$V	5	3.833	21[6]	66[6]	14.92	40.71	0.0551	19.05	51.92	0.0700
$_{6}$C+$_{23}$V	12	3.833	45[6]	124[6]	34.78	94.59	0.1268	51.99	141.24	0.1886
$_{6}$C+$_{24}$Cr	5	4.0	21[6]	78[6]	13.43	36.80	0.0474	16.65	45.55	0.0585
$_{6}$C+$_{24}$Cr	12	4.0	35[6]	136[6]	33.04	90.18	0.1150	49.46	134.79	0.1711
$_{6}$C+$_{25}$Mn	5	4.167	21[6]	72[6]	12.70	34.74	0.0432	14.78	40.35	0.0498
$_{6}$C+$_{25}$Mn	12	4.167	41[6]	120[6]	31.66	86.21	0.1057	47.21	128.36	0.1566
$_{6}$C+$_{26}$Fe	5	4.333	17[6]	63[6]	11.92	32.61	0.0388	13.30	36.34	0.0431
$_{6}$C+$_{26}$Fe	8	4.333	16[5]	80[5]	25.62	69.85	0.0823	34.84	94.87	0.1113
$_{6}$C+$_{26}$Fe	12	4.333	41[6]	111[6]	30.94	84.31	0.0992	46.02	125.20	0.1466
$_{6}$C+$_{26}$Fe	36	4.333	46[5]	140[5]	47.40	129.01	0.1511	63.01	171.38	0.2004
$_{6}$C+$_{27}$Co	5	4.5	14[6]	55[6]	11.29	30.87	0.0353	11.94	32.61	0.0372
$_{6}$C+$_{27}$Co	12	4.5	44[6]	107[6]	30.80	83.85	0.0947	44.85	121.91	0.1371
$_{6}$C+$_{28}$Ni	5	4.667	19[6]	47[6]	10.50	28.76	0.0316	10.43	28.53	0.0314
$_{6}$C+$_{28}$Ni	12	4.667	37[6]	95[6]	29.82	81.32	0.0884	43.11	117.39	0.1269
$_{6}$C+$_{29}$Cu	5	4.833	10[6]	43[6]	10.16	27.89	0.0294	9.63	26.43	0.0279
$_{6}$C+$_{29}$Cu	12	4.833	27[6]	110[6]	29.04	79.38	0.0829	41.22	112.51	0.1168
$_{6}$C+$_{30}$Zn	8	5	13[5]	89[5]	17.65	48.19	0.0489	21.13	57.62	0.0583
$_{6}$C+$_{30}$Zn	36	5	37[5]	130[5]	42.94	116.85	0.1174	61.23	166.46	0.1666
$_{6}$C+$_{47}$Ag	84.5	7.833	–	112±7	27.22	70.84	0.0462	40.45	105.14	0.0681
$_{6}$C+$_{48}$Cd	84.5	8	–	94±5	26.47	68.77	0.0439	39.31	102.04	0.0647
$_{6}$C+$_{49}$In	84.5	8.167	–	96±4	25.72	66.68	0.0416	38.39	99.44	0.0618
$_{6}$C+$_{50}$Sn	84.5	8.333	–	94±3	24.87	64.54	0.0394	37.28	96.45	0.0587

In Table 3, the first column is projectile–target combinations, the second column is the kinetic energy of the incident ions, the third is the ratio of nuclear charge of targets and incidence, and the fourth is the experimental $K\alpha$ and $K\beta$ x-ray energy shifts. Because the BEA scaling function $G(V)$ were slightly different in different approximations, the calculated ionization probability per electron p_{nl} and x-ray energy shifts were slightly different. In Table 3, the fifth column is the calculated ionization probability per electron and K x-ray energy shifts, which were calculated according to the scaling function $G(V)$ suggested by Gryzinski,[20] and the sixth column is calculated results basing on scaling function $G(V)$ of the Gerjuoy *et al*, which includes the Coulomb deflection corrections of projectiles.

From Table 3 it can be seen that 1) the experimental $K\alpha$ and $K\beta$ x-ray energy shifts (or ionization probability) increase as the Z_2/Z_1 decreases when the kinetic energy of incident ions were fixed for the same incident ions; 2) the x-ray energy shifts increase as the kinetic energy of projectile increases for the same projectile–target combination. It inferred that the ionization mechanism of target atom is dominated by the direct Coulomb excitation in the MeV/u heavy-ion collisions; 3) our calculated results are in accordance with the experimental results in some ways except for our experimental $K\alpha$ x-ray spectra.

It can be seen from comparing the values of the fifth column and the sixth column that 1) the x-ray energy shifts calculated according to the scaling function of Gryzinski agreed well with the experimental results at smaller ranges of Z_2/Z_1, otherwise at the larger Z_2/Z_1 ranges, the calculated results basing on scaling function of Gerjuoy *et al* agreed well with the experimental results, which indicate that the Coulomb deflection of projectile is not important and the vacancy rearrangement processes is much more significant at smaller Z_2/Z_1, the distribution of vacancies is no longer described with a binomial distribution at the time of emission of x-ray; 2) the calculated values of $K\beta$ x-ray energy shifts are according more well with the experiments than the case of $K\alpha$ x-ray lines, it is due to the experimental error for $K\alpha$ x-ray is larger than that of $K\beta$ x-ray; and 3) the calculated values of fifth column are slightly smaller than the experimental results especially for larger Z_2/Z_1, it is as a result of not including the Coulomb deflection correction in scaling function $G(V)$, and the contributions of exchange potential energy and electron–nucleus potential energy did not include too as pointed out in Section 2. We just think that this model could estimate the K x-ray energy shifts such that they are relatively accurate for the high energetic incident ions and large Z_2/Z_1 projectile–target combinations in heavy-ion collisions.

5. Conclusions

The model of Burch *et al* for calculating K x-ray energy shifts due to an additional vacancy in $2p$ sub-shell has been extended to calculate K x-ray energy shifts of multiple ionized atoms by MeV/u heavy ions. The model was constructed basing on two sudden approximations: 1) the number of initial vacancies were described by the binomial distribution $P_{2l}(n) = C_N^n p_{2l}^n (1-p_{2l})^{N-n}$; 2) one assumed a constant contribution per an additional vacancy in $2l$ shell to K x-ray energy shifts, and the contributions of vacancies in outer shell, were not instance M and N-shell, did not be included. Moreover the vacancy rearrangement processes during the time from heavy-ion collisions to x-ray emission and the modification of fluorescence yield due to multiple ionization were not considered in this model.

The K x-ray spectra of $_{47}$Ag, $_{48}$Cd, $_{49}$In, and $_{50}$Sn induced by 84.5 MeV carbon ions were measured by an HPGe semiconductor detector. The experiment revealed that the $K\alpha$ x-ray energy shifts were not obvious but the $K\beta$ x-ray lines had about 90∼110 eV energy shifts. In addition to our experimental results, many other experimental results in the literature were examined and compared with the calculated values of the model. The investigative results showed that 1) the dominant ionization mechanism in MeV/u heavy-ion collisions was the direct Coulomb excitation; 2) for approximate symmetry collisions, i.e. at smaller ranges of Z_2/Z_1, the vacancy rearrangement processes became much more considerable than at larger Z_2/Z_1 ranges.

References

[1] Richard Patrick, Morgan I L, Furuta T and Burch D 1969 *Phys. Rev. Lett.* **23** 1009

[2] Burch D and Richard Patrick 1970 *Phys. Rev. Lett.* **25** 983

[3] Li J W, Zhou S H, Hu A D, Zeng X T and Tian W 1996 *Nucl. Sci. Tech.* **7** 238

[4] Mokler P H 1971 *Phys. Rev. Lett.* **26** 811
Briand J P, Chevallier P, Tavernier M and Rozet J P 1971 *Phys. Rev. Lett.* **27** 777
Burch D and Richard Patrick 1971 *Phys. Rev. Lett.* **26** 1355
Burch D, Ingalls W B, Risley J S and Heffner R 1972 *Phys. Rev. Lett.* **29** 1719
Bissinger G A, Baskin A B, Choi B H and Shafroth S M 1972 *Phys. Rev.* A **6** 545
Polasik Marek 1989 *Phys. Rev.* A **39** 616

[5] Wheeler R M, Chaturvedi R P, Duggan J L, Tricomi J and Miller P D 1976 *Phys. Rev.* A **13** 958

[6] Fazinić S, Tadić T, Bogdanović I, Jaksić M, Orlić I and Valković 1996 *Nucl. Inst. Meth.* B **114** 232

[7] Laubert R, Haselton H, Mowat J R, Peterson R S and Sellin I A 1975 *Phys. Rev.* A **11** 135

[8] Ciortea C, Piticu I, Fluerasu D, Dumitriu D E, Enulescu A, Gugiu M M, Radu A T and Penescu L C 2005 *Nucl. Inst. Meth.* B **232** 342

[9] Ciortea C, Dumitriu Dana, Enescu Sanda E, Enulescu A, Fluerasu Daniela, Piticu I and Szilagyi Z S 2002 *Nucl. Inst. Meth.* B **193** 109

[10] Burch D, Wilets L and Meyerhof W E 1974 *Phys. Rev.* A **9** 1007

[11] Roy S K, Ghosh D K and Talukdar B 1983 *Phys. Rev.* A **28** 1169

[12] Bhattacharya J, Datta J and Talukdar B 1985 *Phys. Rev.* A **32** 941

[13] Banas D, Braziewicz J, Majewska U, Pajek M, Semaniak J, Czyzewski T, Jaskola M, Kretschmer W and Mukoyama T 1999 *Nucl. Instr. Meth.* B **154** 247
Banas D, Braziewicz J, Kubala-Kukus A, Majewska U, Pajek M, Semaniak J, Czyzewski T, Jaskola M, Kretschmer W and Mukoyama T 2000 *Nucl. Instr. Meth.* B **164–165** 344
Banas D, Pajek M, Semaniak J, Braziewicz J, Kubala-Kukus A, Majewska U, Czyzewski T, Jaskola M, Kretschmer W, Mukoyama T and Trautmann D 2002 *Nucl. Instr. Meth.* B **195** 233

[14] Bhattacharya J, Talukdar B and Laha U 1989 *Z. Phys.* D **14** 107

[15] Sulik B, Hock G and Berenyi D 1984 *J. Phys.* B **17** 3239
Sulik B, Kadar I, Ricz S, Varga D, Vegh J, Hock G and Berenyi D 1987 *Nucl. Inst. Meth.* B **28** 509

[16] Lapicki G 2007 *Radi. Phys. Chem.* **76** 475

[17] Bearden J A 1967 *Rev. Mod. Phys.* **39** 78

[18] Cowan R D 1981 *The Theory of Atomic Structuce and Spectra* (Berkeley: University of California Press) p214

[19] Witikower A B and Betz H D 1973 *Atomic Data* **5** 113

[20] McGuire J H and Richard P 1973 *Phys. Rev.* A **8** 1374